

1001221 51111
IN-36-CR
170236
P. 36 1

PROGRESS REPORT

SUBMITTED TO :

National Aeronautics and
Space Administration
Langley Research Center
Hampton, Virginia 23665

INSTITUTION:

Department of Physics
Hampton University
Hampton, Virginia 23668

TITLE OF RESEARCH:

Development of Mid-Infrared
Solid State Lasers for
Spaceborne Lidar

NASA GRANT NUMBER:

NAG-1-877

PERIOD COVERED BY THIS REPORT:

April 13, 1988 - October 13, 1988

PRINCIPAL INVESTIGATOR:

Donald A. Whitney

CO-PRINCIPAL INVESTIGATOR:

Kyong H. Kim

(NASA-CR-183341) DEVELOPMENT OF
MID-INFRARED SOLID STATE LASERS FOR
SPACEBORNE LIDAR Semiannual Progress Report,
13 Apr. - 13 Oct. 1988 (Hampton Inst.)
36 p

N89-12053

Unclas
CSCI 20E 63/36 0170236

Summary

This semiannual progress report covers work performed during the period from April 13, 1988 to October 13, 1988 under NASA grant number NAG-1-877 entitled "Development of mid-infrared solid state lasers for spaceborne lidar". We have designed a flashlamp-pumped $\text{Cr}^{3+}:\text{GSAG}$ laser of pulsed laser energy greater than 200 mJ and of pulse width of 1 ms FWHM to simulate a high power laser diode in pumping mid-infrared laser crystals such as Tm^{3+} , Er^{3+} and/or Ho^{3+} -ion doped YAG, YLF or other host materials. This $\text{Cr}^{3+}:\text{GSAG}$ laser will be used to determine optimum conditions for laser diode pumped mid-infrared lasers, maximum energy extraction limit with longitudinal pumping, thermal damage limit, and other problems related to high power laser diode pumping. We have completed a modification of an existing flashlamp-pumped and liquid-nitrogen-cooled rare earth laser system for 60 J electrical input energy and 500 μs pulse width, and have carried out preliminary experiments with a $\text{Ho}^{3+}:\text{Er}^{3+}:\text{Tm}^{3+}:\text{YAG}$ crystal to test the system performance. This flashlamp-pumped rare earth laser system will be used to determine optimum Tm^{3+} -ion concentration in $\text{Ho}^{3+}:\text{Cr}^{3+}:\text{Tm}^{3+}:\text{YAG}$ crystal in the remaining research period.

CONTENTS

	Page
Summary	
I. Flashlamp pumped Cr:GSAG Laser As a High-Power Diode Simulator	
1. Introduction	1
2. Flashlamp Pumped Cr:GSAG Laser	2
II. Experiments on Flashlamp-Pumped Rare Earth Laser System	
1. Introduction	5
2. Flashlamp Pumped Rare Earth Laser Experiments	6
III. Conclusion	9
References	13
List of Figures	15
Appendix	29

I. Flashlamp Pumped Cr:GSAG Laser for Rare Earth Laser Pumping

1. Introduction

During this report period we have designed a flashlamp pumped Cr:GSAG laser to simulate a high power laser diode in pumping rare earth ion (such as Tm^{3+} , Er^{3+} and Ho^{3+}) doped crystals and to study various problems involved with high power laser diode pumping. The diode-pumped solid state laser system has been known as a very promising technology for the spaceborne lidar (light detection and ranging) and windshear lidar applications because of its long system lifetime, reliability, high efficiency, low thermal loading, compactness and low-voltage operation. However, the current technology on the laser diode is not mature especially in high power or high energy applications and its price per unit output power is very high. The reported highest cw laser output from a single array diode is 38 W [Ref.1]. The highest quasi-cw laser output from a one-dimensional bar is 134 W for a pulse width of 150 μs and repetition rate of 40 Hz and that from a two-dimensional stacked bar is 800 W (corresponding power density of 2 kW/cm^2) for the same pulse width and repetition. The flashlamp pumped Cr:GSAG laser can be built with a relatively low cost and can deliver high laser output energies of 200 mJ - 1 J. The corresponding average laser pulse powers are 100 W - 2 kW for 0.2 - 2 ms pulses. In addition, since the wavelength of most currently well-developed laser diodes is located near 800 nm, the Cr:GSAG laser wavelength matches well to the diode wavelength and can be precisely tuned to the absorption peak of the rare earth ions. Since the absorption lines of the Tm^{3+} and Er^{3+} -ions match well with the diode laser wavelength and efficient energy transfer from the Tm^{3+} and Er^{3+} ions to Ho^{3+} ions has been already utilized in low

power laser operation with laser diode pumping as listed in Table 1 [Refs.2-7], high power laser operation of rare earth crystals, such as $\text{Ho}^{3+}:\text{Tm}^{3+}:\text{YAG}$, $\text{Ho}^{3+}:\text{Er}^{3+}:\text{Tm}^{3+}:\text{YAG}$, $\text{Er}:\text{YAG}$ and $\text{Er}:\text{YLF}$, at various wavelengths of $2.1\mu\text{m}$, $2.3\mu\text{m}$ and $2.9\mu\text{m}$ may be expected with high power laser diode pumping. The flashlamp pumped $\text{Cr}:\text{GSAG}$ laser will be used not only to simulate high power laser diode pumps but also to determine an optimum combination of the host and rare earth ions, threshold, slope efficiency, operating temperature and output coupler's reflectance for the efficient rare earth lasers. Furthermore, William E. Krupke predicted that the solid state lasers pumped longitudinally with laser diodes are limited to a maximum deliverable output of 10 W [Ref.8]. The $\text{Cr}:\text{GSAG}$ laser will be useful in determination of the upper limit of the rare earth laser output with a longitudinal pumping at a wavelength which corresponds to diode laser wavelength and absorption peak of the rare earth ions.

In the following sections we will describe the characteristics of the flashlamp pumped $\text{Cr}:\text{GSAG}$ laser and its system design.

2. Flashlamp Pumped $\text{Cr}:\text{GSAG}$ Laser

Fig.1 shows the absorption and fluorescence spectra of the $\text{Cr}:\text{GSAG}$ crystal. The fluorescence spectrum covers well the laser diode wavelength range which is around 780 nm to 850 nm. Previously other research groups [Refs.9,10] have demonstrated tunable laser operation of the crystal in the wavelength range from 765 nm to 800 nm and obtained the maximum laser output of 200 mJ at 780 nm with a pulse width of 150 μs . It is our primary objective to develop a long-pulsed high energy $\text{Cr}:\text{GSAG}$ laser of adjustable pulsed laser energy of 200 mJ to 1 J and pulse width of 0.2 ms to 1 ms at the wavelength of 790 nm.

Typical pulse forming network (PFN) with a single RLC circuit

is shown in Fig.2. According to the Refs.11-13, the design parameters can be calculated using the following relations:

$$C = [2 E_o \alpha^4 T^2 K_o^{-4}]^{1/3}$$

$$K_o = 1.28 l_f / D (p/x)^{1/5}$$

$$L = T^2 / C$$

$$V_o = [2 E_o / C]^{1/2}$$

$$E_x = K_e T^{1/2}$$

$$\tau_{life} = [E_o / E_x]^{-8.5}$$

$$I = (V / K_o)^2$$

$$A = \pi (D / 2)^2$$

$$T_B = [\{ 9450 \times (D/100)^{0.03} (I/A)^{0.01} \}^6 + \{ 93 \times (D/100)^{0.27} (I/A)^{0.34} \}^6]^{1/6}$$

$$\lambda_p = 2.898 \times 10^6 / T_B$$

$$Z_o = [L / C]^{1/2}$$

$$R_t = \rho l_f / A$$

$$I_p = V / (Z_o + R_t)$$

where C is the capacitance of the charging capacitor in Farad, E_o is electrical energy stored in capacitor in Joule, α is damping factor (=0.8 for critical damping), T is circuit time constant (= $T_o/3$), T_o is current pulse width measured at 1/3 of peak in second, K_o is impedance parameter of flashlamp in $\Omega(\text{amp})^{0.5}$, l_f is arc length of the flashlamp in cm, D is flashlamp bore diameter in cm, p is gas fill pressure in flashlamp in Torr, x is a constant (= 450 for Xe-gas, and 805 for Kr-gas), L is inductance in Henry, V_o is initial capacitor voltage in volt, E_x is explosion energy in Joule, K_e is explosion energy constant of the given flashlamp, τ_{life} is flashlamp lifetime in shot number, V and I are instantaneous flashlamp discharge voltage and current in volt and ampere, respectively, A is flashlamp bore cross section in cm^2 . T_B is

blackbody temperature in °K, λ_p is the wavelength at the peak of the blackbody spectrum in nm, Z_o is the impedance of the LC circuit in ohm, R_t is flashlamp resistance, ρ is flashlamp resistivity in $\Omega \cdot \text{cm}$ (0.02 for pulse width between 100 μs and 1 ms pulses), and I_p is the peak current on the discharge circuit. The result of the calculated parameters for ILC model 4F3 flashlamp [$D = 0.4 \text{ cm}$, $l_f = 7.62 \text{ cm}$, $K_o = 25 \Omega(\text{amp})^{0.5}$, $K_e = 7.5 \times 10^4 \text{ Watts}(\text{sec})^{0.5}$, Max $I_p = 500 \text{ A}$] is shown on Table 2. As long as the pulse width is kept long, the lifetime of the flashlamp can be extended even at high input energies.

In order to have long square-wave pulses, pulse forming network with multiple LC series sections has been designed. Design parameters for the multisection PFN circuit can be calculated according to Ref.14 using the same relations and parameters as above unless otherwise specified below:

$$V = 2 [K_o^2 E_o / T_o]^{1/3}$$

$$C = [E_o T_o^2 / K_o^4]^{1/3} / 2$$

$$L = [T_o^4 K_o^4 / E_o]^{1/3} / 2$$

$$C_o = C/n$$

$$L_o = L/n$$

$$\tau_{\text{rise}} \approx [L_o C_o]^{1/2}$$

$$Z_o = [L / C]^{1/2}$$

$$I = V / 2Z_o$$

$$I_p = V / (Z_o + R_t)$$

where n is the number of the LC sections, C is capacitance of total charging capacitors, L is total inductance, C_o and L_o are each sectional capacitance and inductance, respectively, and τ_{rise} is risetime of the square wave pulse. Typical pulse forming network with 3 LC sections is shown in Fig.3 and the calculated parameters for the PFN circuit with the same ILC model 4L3

flashlamp are listed on Table 3. The computer programs used in a HP9845B computer for the above calculations are found in the Appendix. The 3 LC section PFN designed for 300 J input energy and 1 ms pulse width with $C_0 = 150 \mu\text{F}$ and $L = 185 \mu\text{H}$ is being assembled for a preliminary setup in present time, and will be scaled up to higher energy and longer pulse width later.

The experimental arrangement to be used for the rare earth laser system with the flashlamp pumped Cr:GSAG laser pumping is shown in Fig.4. The Cr:GSAG laser will be tuned with an internal prism to the absorption line of rare earth ions near typical diode laser wavelength which is around 790 nm, and then will be focused by a lens to the rare earth ion doped crystal through the highly reflective mirror for the rare earth laser. Narrow line pumping of the rare earth lasers with the Cr:GSAG laser will be useful to study the energy transfer processes and their effect on laser performance, and will enable simulation of high power diode laser pumping. Q-switching experiment will be also performed to study the efficiency of energy transfer mechanisms for short pulse DIAL and Doppler Lidar operation.

II. Flashlamp-Pumped Rare Earth Laser System

1. Introduction

Recently, codoping Cr^{3+} -ions in rare earth ion doped crystals has been demonstrated by many research groups as an effective way to improve efficiency of flashlamp pumped laser systems. Diode-pumped rare earth lasers are promising candidates for the space-borne lidar system in the mid-infrared spectral region. However, we see from the situation of the current technology that the flashlamp pumped laser systems have still several practical advantages over the diode-pumped lasers, although the latter have an order of magnitude higher efficiency and more easily obtain room temperature operation. The major advantages are that the

flashlamp systems are well developed and easily accessible. Especially in high laser energy (or power) applications the technology for the flashlamp pumped laser system is well developed compared to that for the diode lasers and capable to deliver a high laser energy (or power) at a relatively low cost. Thus, understanding of the mechanisms of the energy transfer processes between the chromium ions and rare earth ions such as Tm^{3+} , Ho^{3+} and Er^{3+} is very important to determine optimum doping concentrations and a proper host material, and to increase the laser efficiency. During this report period we have prepared for the flashlamp pumped and liquid nitrogen cooled rare earth laser system, which is shown in Fig.5, to study the laser characteristics of three $\text{Ho}^{3+}:\text{Cr}^{3+}:\text{Tm}^{3+}:\text{YAG}$ crystals provided by Coherent Laser Technology Company and to determine the optimum Tm^{3+} concentration in the $\text{Ho}^{3+}:\text{Cr}^{3+}:\text{Tm}^{3+}:\text{YAG}$ crystals.

2. Flashlamp Pumped Rare Earth Laser Experiment

Fig.5 shows the typical energy transfer processes among Ho^{3+} , Cr^{3+} and Tm^{3+} ions in the YAG crystal. The broad $^4\text{T}_1$ and $^4\text{T}_2$ states of the Cr^{3+} -ions provide an efficient absorption of the flashlamp light and energy transfer takes place from the $^4\text{T}_1$ state of the Cr^{3+} -ion to the $^3\text{H}_4$ state of the Tm^{3+} -ion and from the $^4\text{T}_1$ state to the $^3\text{H}_4$ through a cascade transition to the $^4\text{T}_2$ state. Then, when the Tm^{3+} ions in the $^3\text{H}_4$ state make transitions to the $^3\text{F}_4$ state, the transition energy is used to excite another Tm^{3+} -ion from the ground state to the $^3\text{F}_4$ state. This, so called cross-relaxation phenomenon, will provide two excited Tm^{3+} ions for one single pump photon by increasing the quantum efficiency to 2. Then the excited Tm^{3+} ions transfer to the $^5\text{I}_7$ state of the Ho^{3+} ions and the $2.1\ \mu\text{m}$ laser transition takes place between the $^5\text{I}_7$ and $^5\text{I}_8$ states of the Ho^{3+} ions. Since the crystals provided by Coherent Laser Technology Company have different Tm^{3+} -ion concentrations with fixed Cr^{3+} and

Tm³⁺-ion concentrations, the normal mode and Q-switched laser study on those crystals at various operating temperatures as well as the spectroscopic study will provide information on the energy transfer processes among those three ions and enable us to determine optimum Tm³⁺-ion concentration in the Ho³⁺:Cr³⁺:Tm³⁺:YAG crystal for the best flashlamp pumped and Q-switched 2.1 μ m laser performance.

In order to test the system performance we have taken normal mode laser operation of a Ho³⁺:Er³⁺:Tm³⁺:YAG crystal under flashlamp pumping at various operating temperatures and with various output mirror reflectivities. The crystal had a doping concentration of 0.02 Ho³⁺, 0.40 Er³⁺ and 0.06 Tm³⁺, and its dimension was 5 mm in diameter and 90 mm in length. A single LC section pulse forming network of C = 146.5 μ F and L = 184 μ H was used to generate discharge pulses with current pulse width of 500 μ s (= T₀) at the capacitor charging voltage of 909 volts (= V₀) at which the corresponding electrical input energy was 60 J (= E₀). The normal mode laser output energy as a function of the electrical input energy were measured at various operating temperatures with a 95% and 98% reflective output mirrors, respectively, as shown in Figs.7 and 8. As the operating temperature was decreased, the slope efficiency was increased and the threshold energy was decreased. The various electrical input energies were obtained by changing the charging voltage. Fig.9 shows the normal mode laser output of the same crystal obtained with various output mirror reflectivities as a function of the electrical input energy at the operating temperature of 170 °K. The normal mode laser output measurement was taken without the Q-switch crystal and polarizer in the experimental setup shown in Fig.5, and the resonator length was 91 cm.

Finally, the normal mode laser output was measured with a 2.17 mm thick ZnSe plate placed at the Brewster angle (= 67.8°) in the normal mode laser resonator to measure the optical loss caused

by the ZnSe polarizer. Figs.10 and 11 show the difference of the normal mode laser output between without and with ZnSe plate in the resonator. Optical loss in the ZnSe plate could be estimated by observing the variation of the slope efficiency with mirror reflectivity. The slope efficiency σ_s is assumed to vary with the output mirror reflectivity R_m according to Ref.16 as

$$\sigma_s = \sigma_{sm} \ln(R_m) / \ln(R_m R_L)$$

where R_L is a fictitious mirror reflectivity representing the losses in the system and σ_{sm} is the maximum slope efficiency obtainable from the material. R_L is related to the losses L in the system as $R_L = 1 - L$. The above equation can be rewritten as

$$1/\sigma_s = (-\ln R_L / \sigma_{sm}) (-1/\ln R_m) + (1/\sigma_{sm}).$$

The inverse slope efficiency is plotted as a function of $-1/\ln R_m$ in Fig.12 using the data shown in Figs.10 and 11. From the slopes and y-intercepts of the two lines, each corresponding to results obtained with and without ZnSe plate in the resonator, respectively, we obtain $R_L = \exp(-20.868/64.681) = 0.72425$ for the case of the ZnSe plate placed in the resonator and $R_L = \exp(-16.953/78.465) = 0.80569$. Thus, the loss coefficient of the ZnSe plate is calculated as $\alpha = L_{\text{with}} - L_{\text{without}} = (1 - R_{L \text{ with}}) - (1 - R_{L \text{ without}}) = 0.081$ (or $0.081/0.217 \text{ cm} = .375 \text{ cm}^{-1}$). This means that the ZnSe plate causes only 8% loss of the laser efficiency.

Table 2. Calculated Parameters for Single-LC-Section Pulse Forming Network.

FLASHLAMP PULSE FORMING NETWORK								
PULSE ENERGY J	PULSE WIDTH μSEC	CAPACI. F	INDUCT. H	VOLT V	EXPLO. ENERGY J	LIFE (10 ⁻⁶)	BLKBDY TEMP. K	PEAK WAVELEN. nm
100	100	6.15E-05	1.81E-05	1802.8	433.0	25.7E-02	8906	325.4
	200	9.77E-05	4.55E-05	1430.9	612.4	48.9E-01	8865	326.9
	300	1.28E-04	7.81E-05	1250.0	750.0	27.4E+00	8841	327.8
	400	1.55E-04	1.15E-04	1135.7	866.0	93.1E+00	8824	328.4
	500	1.80E-04	1.54E-04	1054.3	968.2	24.0E+01	8811	328.9
	600	2.03E-04	1.97E-04	992.1	1060.7	52.2E+01	8800	329.3
	700	2.25E-04	2.42E-04	942.4	1145.6	10.0E+02	8791	329.7
	800	2.46E-04	2.89E-04	901.4	1224.7	17.7E+02	8783	330.0
	900	2.66E-04	3.38E-04	866.7	1299.0	29.2E+02	8776	330.2
	1000	2.86E-04	3.89E-04	836.8	1369.3	45.7E+02	8770	330.4
200	100	7.75E-05	1.43E-05	2271.4	433.0	71.0E-05	8947	323.9
	200	1.23E-04	3.61E-05	1802.8	612.4	13.5E-03	8906	325.4
	300	1.61E-04	6.20E-05	1574.9	750.0	75.7E-03	8882	326.3
	400	1.95E-04	9.10E-05	1430.9	866.0	25.7E-02	8865	326.9
	500	2.27E-04	1.23E-04	1328.3	968.2	66.4E-02	8851	327.4
	600	2.56E-04	1.56E-04	1250.0	1060.7	14.4E-01	8841	327.8
	700	2.84E-04	1.92E-04	1187.4	1145.6	27.7E-01	8832	328.1
	800	3.10E-04	2.29E-04	1135.7	1224.7	48.9E-01	8824	328.4
	900	3.35E-04	2.68E-04	1092.0	1299.0	80.7E-01	8817	328.7
	1000	3.60E-04	3.09E-04	1054.3	1369.3	12.6E+00	8811	328.9
300	100	8.88E-05	1.25E-05	2600.1	433.0	22.6E-06	8971	323.0
	200	1.41E-04	3.15E-05	2063.7	612.4	43.1E-05	8930	324.5
	300	1.85E-04	5.42E-05	1802.8	750.0	24.1E-04	8906	325.4
	400	2.24E-04	7.95E-05	1638.0	866.0	81.9E-04	8889	326.0
	500	2.60E-04	1.07E-04	1520.6	968.2	21.2E-03	8875	326.5
	600	2.93E-04	1.36E-04	1430.9	1060.7	45.9E-03	8865	326.9
	700	3.25E-04	1.68E-04	1359.2	1145.6	88.4E-03	8855	327.3
	800	3.55E-04	2.00E-04	1300.1	1224.7	15.6E-02	8848	327.5
	900	3.84E-04	2.34E-04	1250.0	1299.0	25.7E-02	8841	327.8
	1000	4.12E-04	2.70E-04	1206.9	1369.3	40.2E-02	8834	328.0
400	100	9.77E-05	1.14E-05	2861.8	433.0	19.6E-07	8988	322.4
	200	1.55E-04	2.87E-05	2271.4	612.4	37.3E-06	8947	323.9
	300	2.03E-04	4.92E-05	1984.3	750.0	20.9E-05	8923	324.8
	400	2.46E-04	7.22E-05	1802.8	866.0	71.0E-05	8906	325.4
	500	2.86E-04	9.73E-05	1673.6	968.2	18.3E-04	8892	325.9
	600	3.23E-04	1.24E-04	1574.9	1060.7	39.8E-04	8882	326.3
	700	3.57E-04	1.52E-04	1496.0	1145.6	76.6E-04	8872	326.6
	800	3.91E-04	1.82E-04	1430.9	1224.7	13.5E-03	8865	326.9
	900	4.23E-04	2.13E-04	1375.8	1299.0	22.3E-03	8858	327.2
	1000	4.53E-04	2.45E-04	1328.3	1369.3	34.9E-03	8851	327.4
500	100	1.05E-04	1.06E-05	3082.8	433.0	29.4E-08	9002	321.9
	200	1.67E-04	2.66E-05	2446.8	612.4	56.0E-07	8960	323.4
	300	2.19E-04	4.57E-05	2137.5	750.0	31.4E-06	8936	324.3
	400	2.65E-04	6.70E-05	1942.0	866.0	10.7E-05	8919	324.9
	500	3.08E-04	9.03E-05	1802.8	968.2	27.5E-05	8906	325.4
	600	3.47E-04	1.15E-04	1696.5	1060.7	59.7E-05	8895	325.8
	700	3.85E-04	1.41E-04	1611.5	1145.6	11.5E-04	8886	326.1
	800	4.21E-04	1.69E-04	1541.4	1224.7	20.3E-04	8878	326.4
	900	4.55E-04	1.98E-04	1482.0	1299.0	33.5E-04	8871	326.7
	1000	4.88E-04	2.27E-04	1430.9	1369.3	52.4E-04	8865	326.9

III. Conclusion

We have calculated pulse forming network parameters for long square-wave typed flashlamp pulse generation and have prepared for construction of a flashlamp-pumped Cr^{3+} :GSAG laser of pulsed laser grater than 200 mJ and of pulse width of 1 ms FWHM. This Cr:GSAG laser will be used to pump 2 - 3 μm lasers using mid-infrared laser crystals such as Tm^{3+} , Er^{3+} and/or Ho^{3+} -ion doped YAG, YLF or other host materials. We have also completed a modification of an existing flashlamp-pumped and liquid-nitrogen-cooled rare earth laser system for 60 J electrical input energy and 500 μs pulse width to determine optimum Tm^{3+} -ion concentration in Ho^{3+} : Cr^{3+} : Tm^{3+} :YAG crystal, and have carried out preliminary experiments with a Ho^{3+} : Er^{3+} : Tm^{3+} :YAG crystal to test the system performance. The slope efficiency of the Ho^{3+} : Er^{3+} : Tm^{3+} :YAG laser increased as the operating temperature decreased and the highest slope efficiency obtained with a 60% reflective mirror was 0.88%. The optical loss coefficient of a 2.17 mm thick ZnSe plate placed at the Brewster angle in the laser resonator as a polarizer was measured to be 0.0814.

Table1. Laser Diode Pumped Rare Earth Laser Work Done By Others In 2 - 3 μm Range

<u>Material</u>	<u>Ion Con- centration</u>	<u>Laser λ</u>	<u>Diode Power</u>	<u>Laser Output</u>	<u>Threshold</u>	<u>Slope[*] Efficiency</u>	<u>Reference</u>
Tm,Ho:YLF	1.5 % Tm	2.31 μm (Tm)	21mW	5.5 mW	10.5 mW	42 %	ref.2
	0.2 % Ho	2.08 μm (Ho)	@791 nm		3.1 mW	26 %	
Tm,Ho:YAG	5.7 % Tm	2.1 μm	100 mW	2.7 mW	3.8 mW	17 %	ref. 3
	0.36% Ho				absorbed		
Cr,Tm,Ho:YAG	2.5x10 ²⁰ cm ⁻³ Cr	2.1 μm		1.2 mW	4.4 mW	19%	ref. 4
	8 x 10 ²⁰ cm ⁻³ Tm				absorbed		
	5 x 10 ¹⁹ cm ⁻³ Ho						
Er,Tm,Ho:YLF (at T=77°K)	1 at wt % Ho	2.06 μm	200 mW	20 mW	5 mW	20 %	ref. 5
	50 % Er	@ 784 nm				(Conversion efficiency)	
Er,Tm,Ho:YAG (at T=77°K)	12 % Tm					19 %	ref. 6
	60 % Er	2.1 μm	100 mW	5.6 mW	40 mW		
Er:YLF	3 % Tm		@ 785.5 nm				
	2 % Ho						
	8 % Er	2.8 μm	200 mW		147 mW	0.7 %	ref. 7

* with respect to absorbed pump power.

Table 3. Calculated Parameters for Multi-LC-Section Pulse Forming Network.

MULTISECTION PULSE FORMING NETWORKS							ORIGINAL PAGE IS OF POOR QUALITY		
INPUT ENERGY J	PULSE WIDTH usec	TOTAL CAPACI. F	TOTAL INDUCT. H	VOLT. V	SECTION CAPACI. F	SECTION INDUCT. H	RISE TIME usec	PEAK CURREN A	BLKBODY TEMP. K
100	200	1.06E-04	9.41E-05	1372	3.54E-05	3.14E-05	33	637	8732
	400	1.69E-04	2.37E-04	1089	5.62E-05	7.90E-05	67	454	8692
	600	2.21E-04	4.07E-04	951	7.37E-05	1.36E-04	100	370	8669
	800	2.68E-04	5.97E-04	864	8.93E-05	1.99E-04	133	319	8652
	1000	3.11E-04	8.04E-04	802	1.04E-04	2.68E-04	167	284	8639
	1200	3.51E-04	1.03E-03	755	1.17E-04	3.42E-04	200	258	8629
	1400	3.89E-04	1.26E-03	717	1.30E-04	4.20E-04	233	238	8620
	1600	4.25E-04	1.51E-03	686	1.42E-04	5.02E-04	267	222	8612
	1800	4.60E-04	1.76E-03	659	1.53E-04	5.87E-04	300	208	8605
	2000	4.93E-04	2.03E-03	637	1.64E-04	6.76E-04	333	196	8599
200	200	1.34E-04	7.47E-05	1728	4.46E-05	2.49E-05	33	882	8773
	400	2.13E-04	1.88E-04	1372	7.09E-05	6.27E-05	67	637	8732
	600	2.79E-04	3.23E-04	1198	9.29E-05	1.08E-04	100	523	8709
	800	3.37E-04	4.74E-04	1089	1.12E-04	1.58E-04	133	454	8692
	1000	3.92E-04	6.38E-04	1011	1.31E-04	2.13E-04	167	406	8679
	1200	4.42E-04	8.14E-04	951	1.47E-04	2.71E-04	200	370	8669
	1400	4.90E-04	1.00E-03	903	1.63E-04	3.33E-04	233	342	8660
	1600	5.36E-04	1.19E-03	864	1.79E-04	3.98E-04	267	319	8652
	1800	5.79E-04	1.40E-03	831	1.93E-04	4.66E-04	300	300	8645
	2000	6.22E-04	1.61E-03	802	2.07E-04	5.36E-04	333	284	8639
300	200	1.53E-04	6.52E-05	1978	5.11E-05	2.17E-05	33	1060	8797
	400	2.43E-04	1.64E-04	1570	8.11E-05	5.48E-05	67	772	8756
	600	3.19E-04	2.82E-04	1372	1.06E-04	9.41E-05	100	637	8732
	800	3.86E-04	4.14E-04	1246	1.29E-04	1.38E-04	133	554	8716
	1000	4.48E-04	5.58E-04	1157	1.49E-04	1.86E-04	167	497	8703
	1200	5.06E-04	7.11E-04	1089	1.69E-04	2.37E-04	200	454	8692
	1400	5.61E-04	8.73E-04	1034	1.87E-04	2.91E-04	233	420	8683
	1600	6.13E-04	1.04E-03	989	2.04E-04	3.48E-04	267	393	8675
	1800	6.63E-04	1.22E-03	951	2.21E-04	4.07E-04	300	370	8669
	2000	7.12E-04	1.41E-03	918	2.37E-04	4.68E-04	333	351	8663
400	200	1.69E-04	5.93E-05	2177	5.62E-05	1.98E-05	33	1206	8813
	400	2.68E-04	1.49E-04	1728	8.93E-05	4.98E-05	67	882	8773
	600	3.51E-04	2.56E-04	1510	1.17E-04	8.55E-05	100	730	8749
	800	4.25E-04	3.76E-04	1372	1.42E-04	1.25E-04	133	637	8732
	1000	4.93E-04	5.07E-04	1273	1.64E-04	1.69E-04	167	572	8719
	1200	5.57E-04	6.46E-04	1198	1.86E-04	2.15E-04	200	523	8709
	1400	6.17E-04	7.94E-04	1138	2.06E-04	2.65E-04	233	485	8700
	1600	6.75E-04	9.48E-04	1089	2.25E-04	3.16E-04	267	454	8692
	1800	7.30E-04	1.11E-03	1047	2.43E-04	3.70E-04	300	428	8685
	2000	7.83E-04	1.28E-03	1011	2.61E-04	4.26E-04	333	406	8679
500	200	1.82E-04	5.50E-05	2345	6.06E-05	1.83E-05	33	1330	8827
	400	2.89E-04	1.39E-04	1862	9.62E-05	4.62E-05	67	976	8786
	600	3.78E-04	2.38E-04	1626	1.26E-04	7.93E-05	100	810	8762
	800	4.58E-04	3.49E-04	1478	1.53E-04	1.16E-04	133	708	8745
	1000	5.32E-04	4.70E-04	1372	1.77E-04	1.57E-04	167	637	8732
	1200	6.00E-04	6.00E-04	1291	2.00E-04	2.00E-04	200	583	8722
	1400	6.65E-04	7.37E-04	1226	2.22E-04	2.46E-04	233	541	8713
	1600	7.27E-04	8.80E-04	1173	2.42E-04	2.93E-04	267	507	8705
	1800	7.86E-04	1.03E-03	1128	2.62E-04	3.43E-04	300	478	8698
	2000	8.44E-04	1.19E-03	1089	2.81E-04	3.95E-04	333	454	8692

References

1. Donald R. Scifres, "Frontiers of semiconductor lasers," CLEO'88, Session MK3, Anaheim, CA (April, 1988).
2. G. Kintz, L. Esterowitz, and R. Allen, "Cascade Laser Emission at 2.31 and 2.08 μm from Laser-Diode Pumped Tm, Ho:LiYF_4 at Room Temperature," Topical Meeting on Tunable Solid State Lasers, Session MC2 (1987).
3. G. J. Kintz, L. Esterowitz, and R. Allen, "CW Diode-Pumped $\text{Tm}^{3+}, \text{Ho}^{3+}:\text{YAG}$ 2.1 μm Room-Temperature Laser," Electronics Lett., 23 (12), 616 (1987).
4. T. Y. Fan, G. Huber, R. L. Byer, and P. Mitzscherlich, "Continuous-wave Operation at 2.1 μm of a Diode-Laser-Pumped, Tm -Sensitized $\text{Ho:Y}_3\text{Al}_5\text{O}_{12}$ laser at 300 K," Opt. Lett. 12 (9), 678 (1987), and CLEO '87, Session FL1 (1987).
5. H. Hemmati, "Diode Laser-pumped Ho:YLF Laser," CLEO '87, Session W14 (1987).
6. R. Allen, L. Esterowitz, L. Goldberg, J. F. Weller, and M. Storm, "Diode-Pumped 2 μm Holmium Laser," Electronics Lett. 22 (18), 947 (1988).
7. G. J. Kintz, R. Allen, and L. Esterowitz, "CW and Pulsed 2.8 μm Laser Emission From Diode-Pumped $\text{Er}^{3+}:\text{LiYF}_4$ at Room Temperature," Appl. Phys. Lett. 50 (22), 1553 (1987).
8. William F. Krupke, "Semiconductor laser-diode-pumped solid-

state laser: status and future," CLEO '88, Session THB1, Anaheim, CA, (April 1988).

9. J. V. Meier, N. P. Barnes, D. K. Remelius, and M. R. Kokta, "Flashlamp-Pumped Cr^{3+} :GSAG Laser," IEEE J. Quantum Electron. QE-22 (10), 2058 (1986).
10. J. Drube, G. Huber, U. Hamburg, and D. Mateika, "Efficiency and tunability of flashlamp-pumped Cr^{3+} :GSAG lasers," CLEO '86, Session THB4, San Francisco, CA (June 1986).
11. ILC Technology Company Technical Bulletins (1 & 2) and Catalog on Flashlamps, 399 Java Dr., Sunnyvale, CA 94089, (1980).
12. EG&G Electro-Optics' Technical Bulletin, "Flashlamp Application Manual," 35 Congress St., Salem, MA 01970, (1986).
13. J. P. Markiewicz and J. L. Emmett, "Design of Flashlamp Driving Circuits," IEEE J. Quantum Electron., QE-2 (11), 707 (1966).
14. Barry Smith, "Overview of flashlamps and arc lamps," SPIE vol. 609, Flashlamp Pumped Laser Technology, page 1 (1986).
15. Michael D. Williams, by private communication.
16. N. P. Barnes, D. J. Gettemy, L. Esterowitz and R. E. Allen, "Comparison of Nd 1.06 and 1.33 μm Operation in Various Hosts," IEEE J. Quantum Electron. QE-23 (9), 1434 (1987).

List of Figures

- Figure 1. Absorption and Fluorescence Spectra of Cr:GSAG Crystal.
- Figure 2. Pulse Forming Network with a Single LC Section.
- Figure 3. Pulse Forming Network with Multiple LC Sections.
- Figure 4. Experimental Arrangement of Flashlamp-Pumped Cr:GSAG Laser for Rare Earth Laser Pumping.
- Figure 5. Experimental Setup for Flashlamp-Pumped and Liquid Nitrogen Cooled Rare Earth Laser System.
- Figure 6. Typical Energy Transfer Processes in $\text{Ho}^{3+}:\text{Cr}^{3+}:\text{Tm}^{3+}:\text{YAG}$ Crystal.
- Figure 7. Normal mode laser output energy of Ho:Er:Tm:YAG crystal as a function of electrical input energy at various operating temperatures with a 95% reflective output mirror.
- Figure 8. Normal mode laser output energy of Ho:Er:Tm:YAG crystal as a function of electrical input energy at various operating temperatures with a 98% reflective output mirror.
- Figure 9. Normal mode laser output of Ho:Er:Tm:YAG crystal as a function of electrical input energy with various output mirrors at an operating temperature of 170 K.
- Figure 10. Loss coefficient measurement of ZnSe plate in a

Ho:Er:Tm:YAG laser resonator with output mirrors of reflectivities of 60% and 95%.

Figure 11. Loss coefficient measurement of ZnSe plate in a Ho:Er:Tm:YAG laser resonator with output mirrors of reflectivities of 80% and 98%.

Figure 12. Inverse slope efficiency versus $-1/\ln R_m$ with and without ZnSe plate in a flashlamp-pumped Ho:Er:Tm:YAG laser.

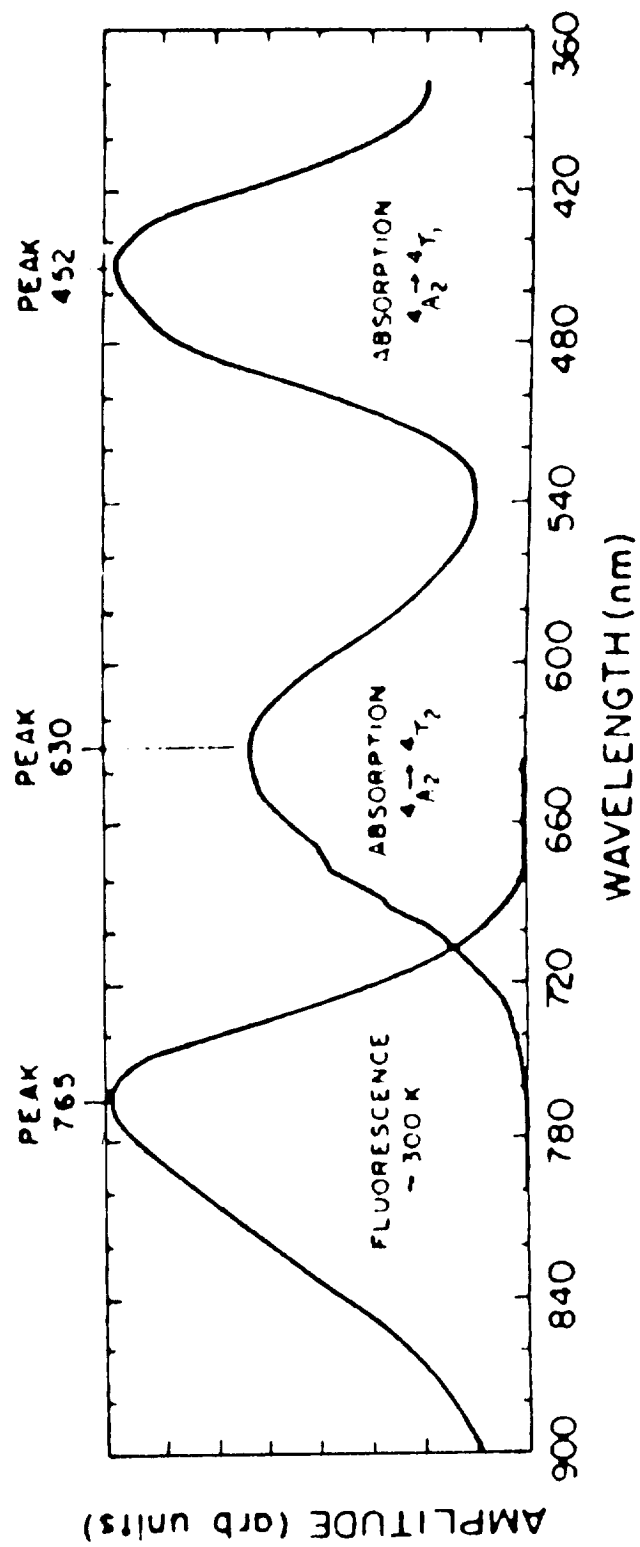


Figure 1. Absorption and Fluorescence Spectra of Cr:GSAG Crystal.

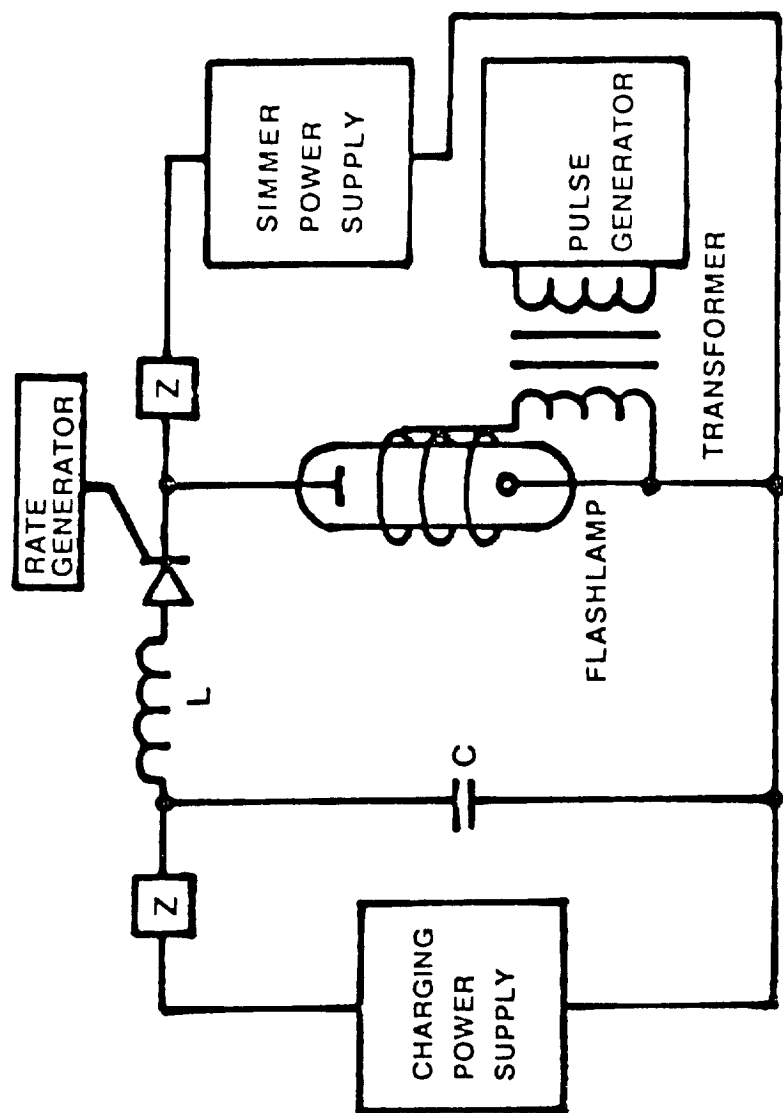


Figure 2. Pulse Forming Network with a Single LC Section.

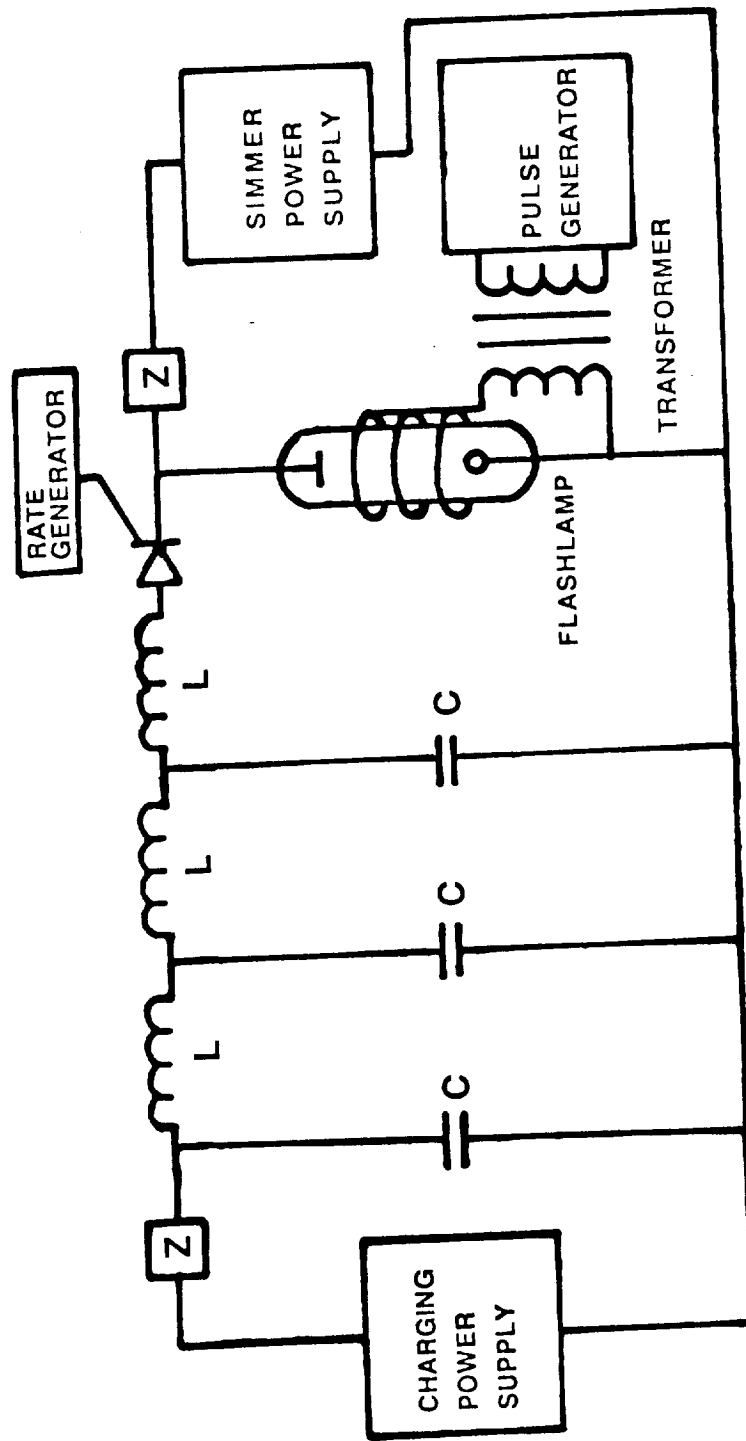


Figure 3. Pulse Forming Network with Multiple LC Sections.

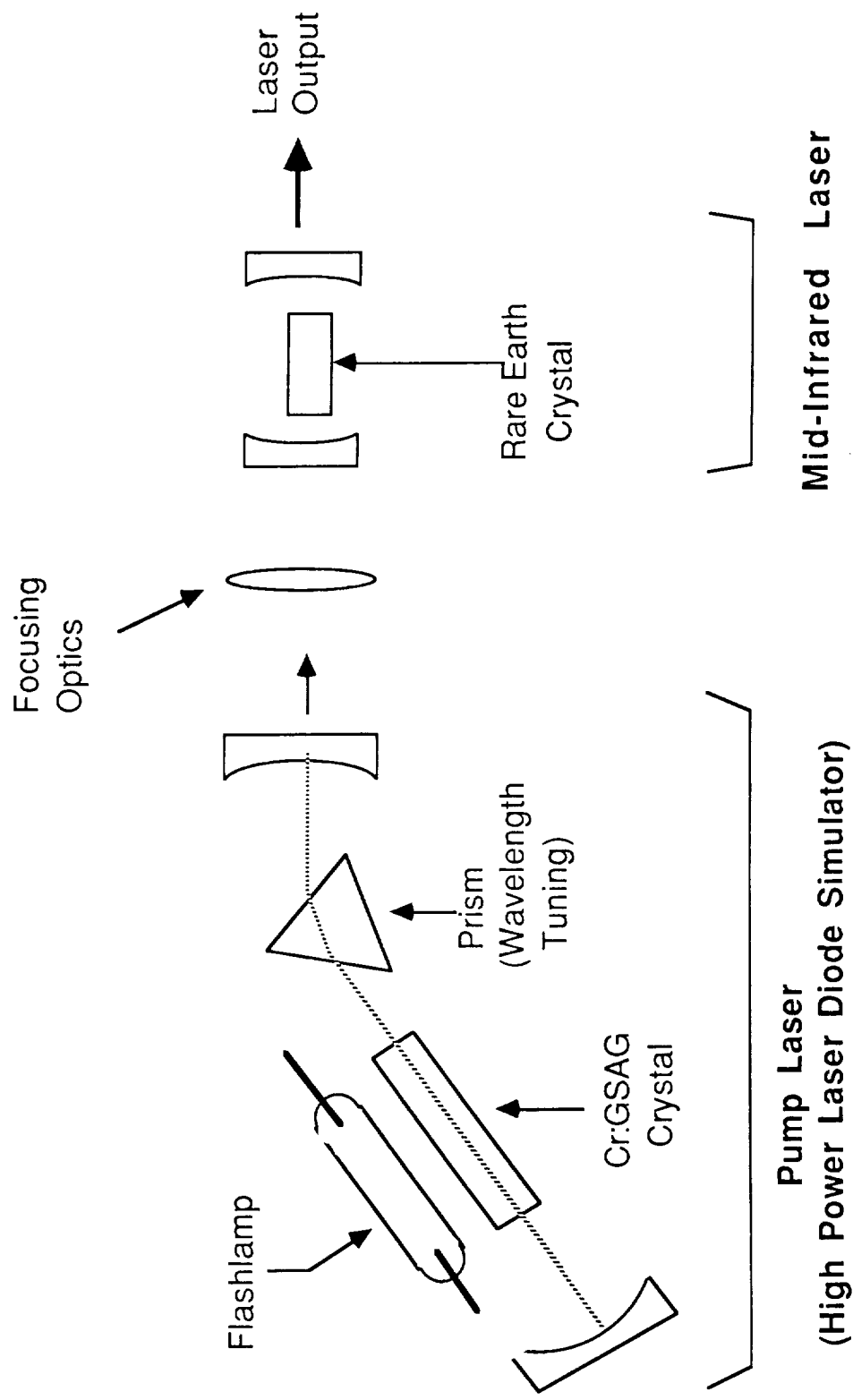


Figure 4. Experimental Arrangement of Flashlamp-Pumped Cr:GSAG Laser for Rare Earth Laser Pumping.

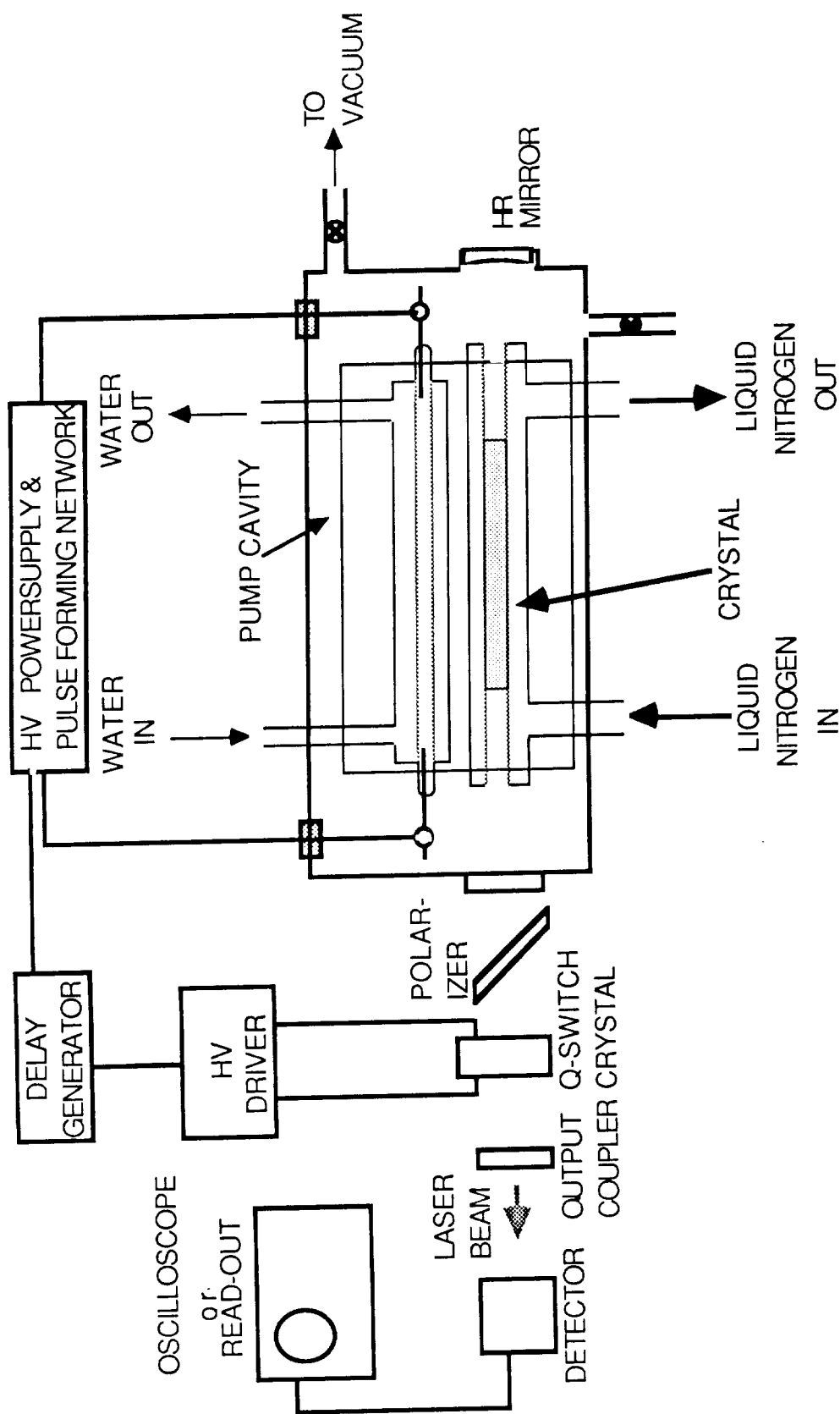


Figure 5. Experimental Setup for Flashlamp-Pumped and Liquid Nitrogen Pumped Rare Earth Laser System.

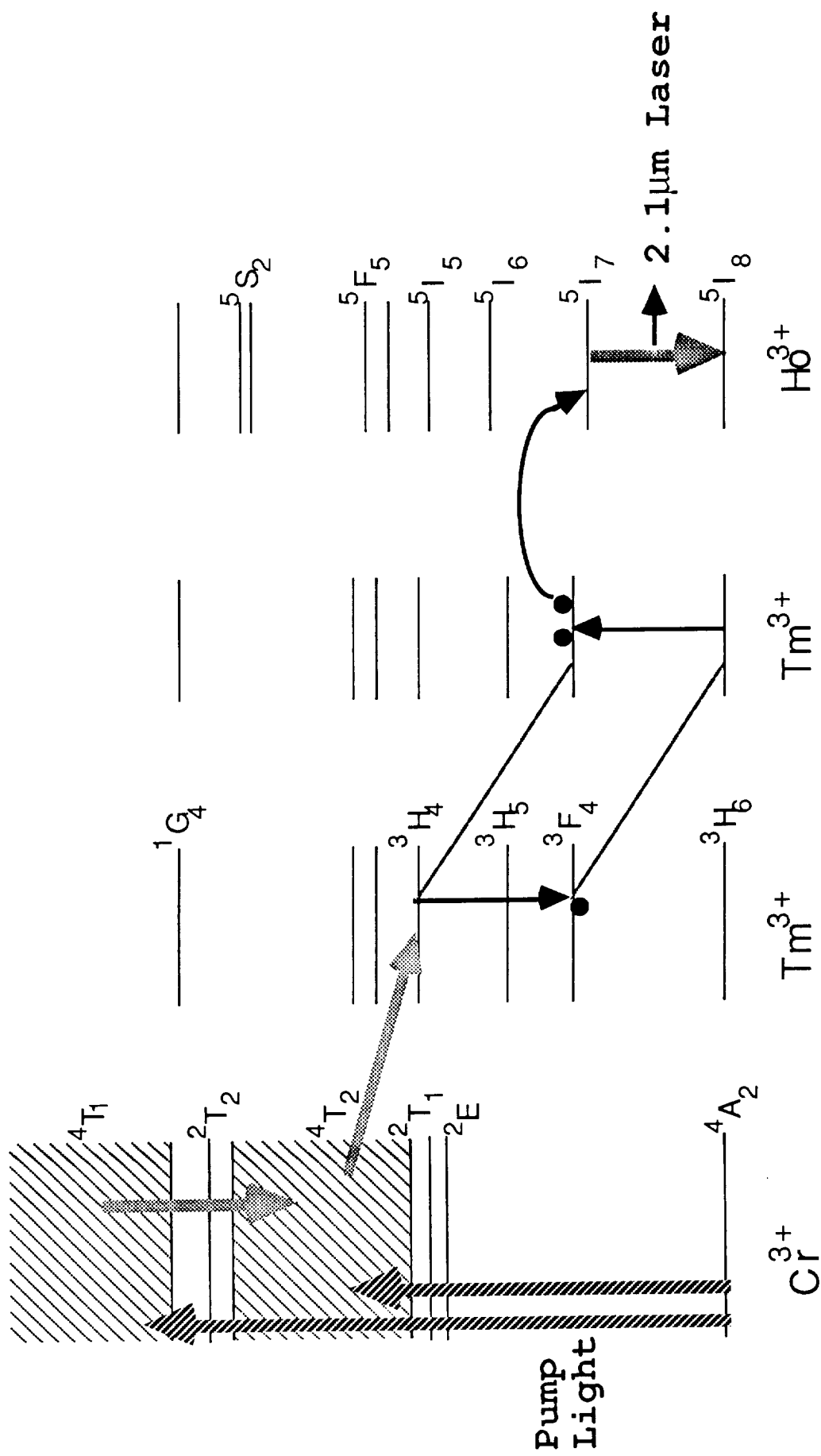


Figure 6. Typical energy transfer processes in $\text{Ho}^{3+}:\text{Cr}^{3+}:\text{Tm}^{3+}:\text{YAG}$ crystal.

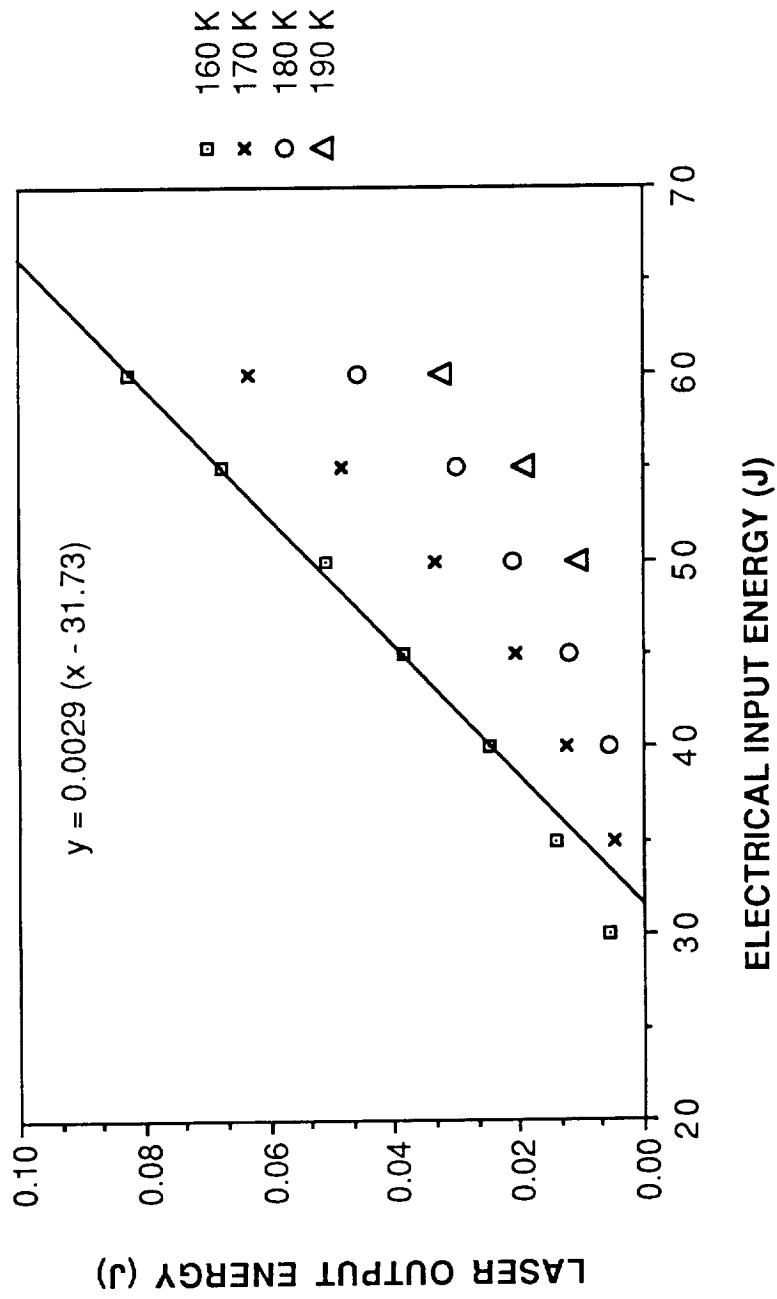


Figure 7. Normal mode laser output energy of Ho:Er:Tm:YAG crystal as a function of electrical input energy at various operating temperatures with a 95 % reflective output mirror.

(0.02 Ho, 0.40 Er, 0.06 Tm), 5 mm x 90 mm rod, C=146.5 μ F, L=184 μ H, Flashlamp pulse width (FWHM) = 300 μ s.

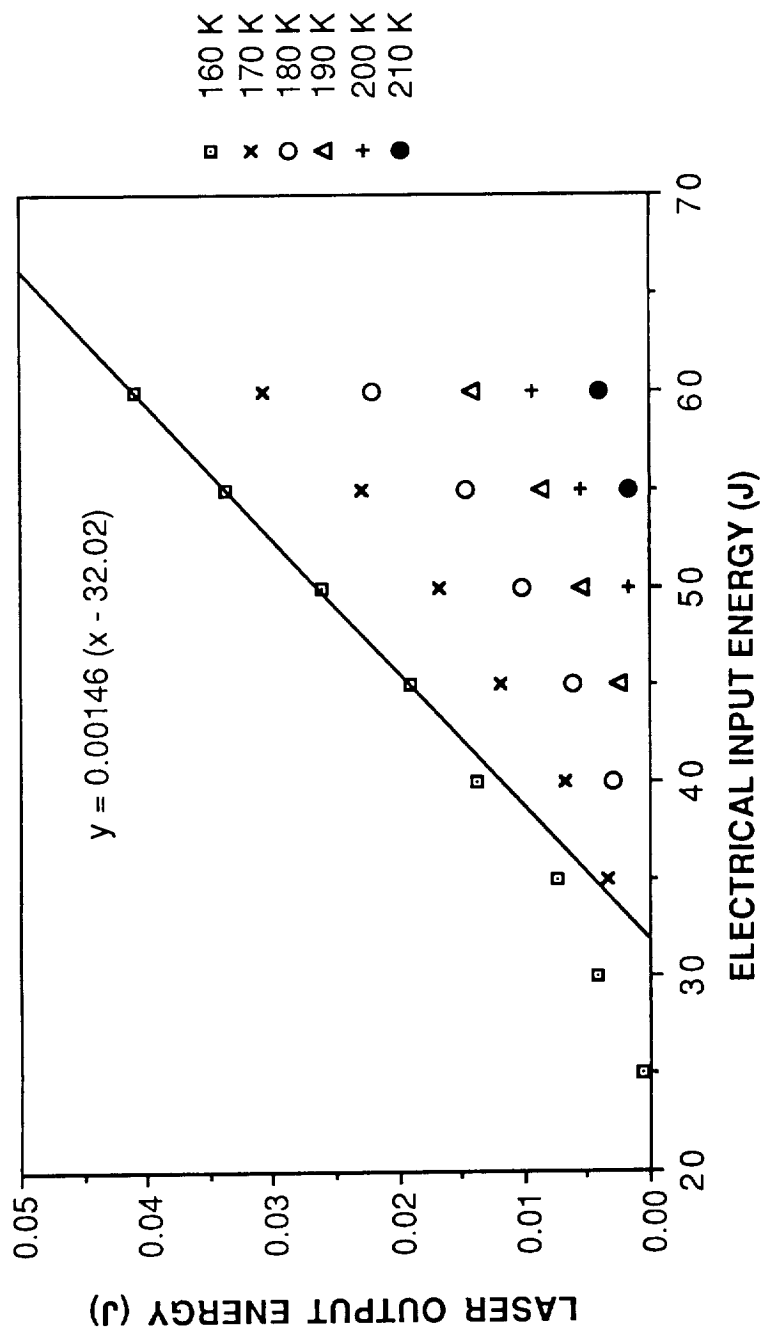


Figure 8. Normal mode laser output energy of Ho:Er:Tm:YAG crystal as a function of electrical input energy at various operating temperatures with a 98% reflective output mirror.

(0.02 Ho, 0.40 Er, 0.06 Tm), 5 mm x 90 mm rod, C=146.5 μ F, L=184 μ H, Flashlamp pulse width (FWHM) = 300 μ s.

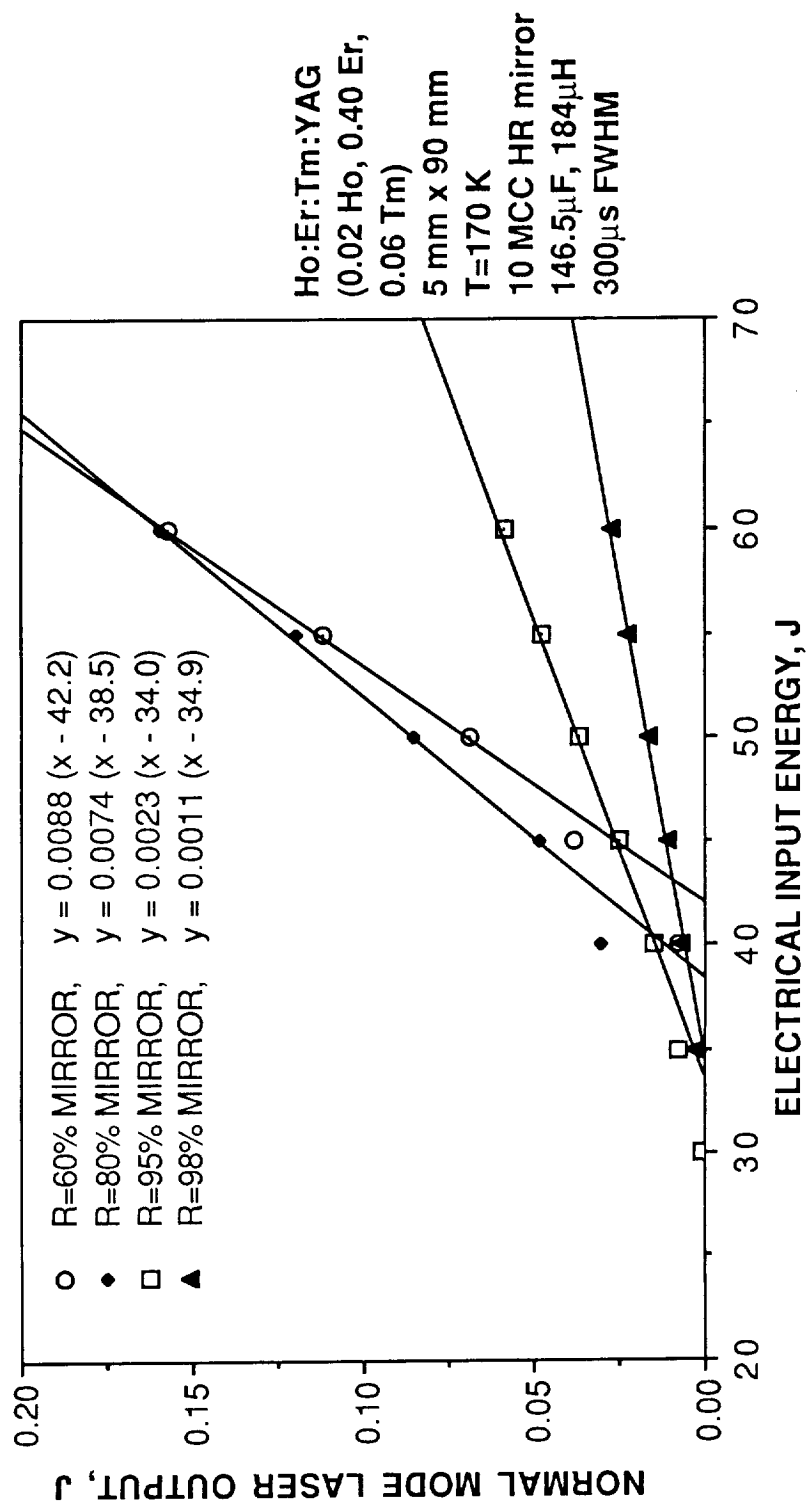


Figure 9. Normal mode laser output of Ho:Er:Tm:YAG crystal as a function of electrical input energy with various output mirrors at an operating temperature of 170 K.

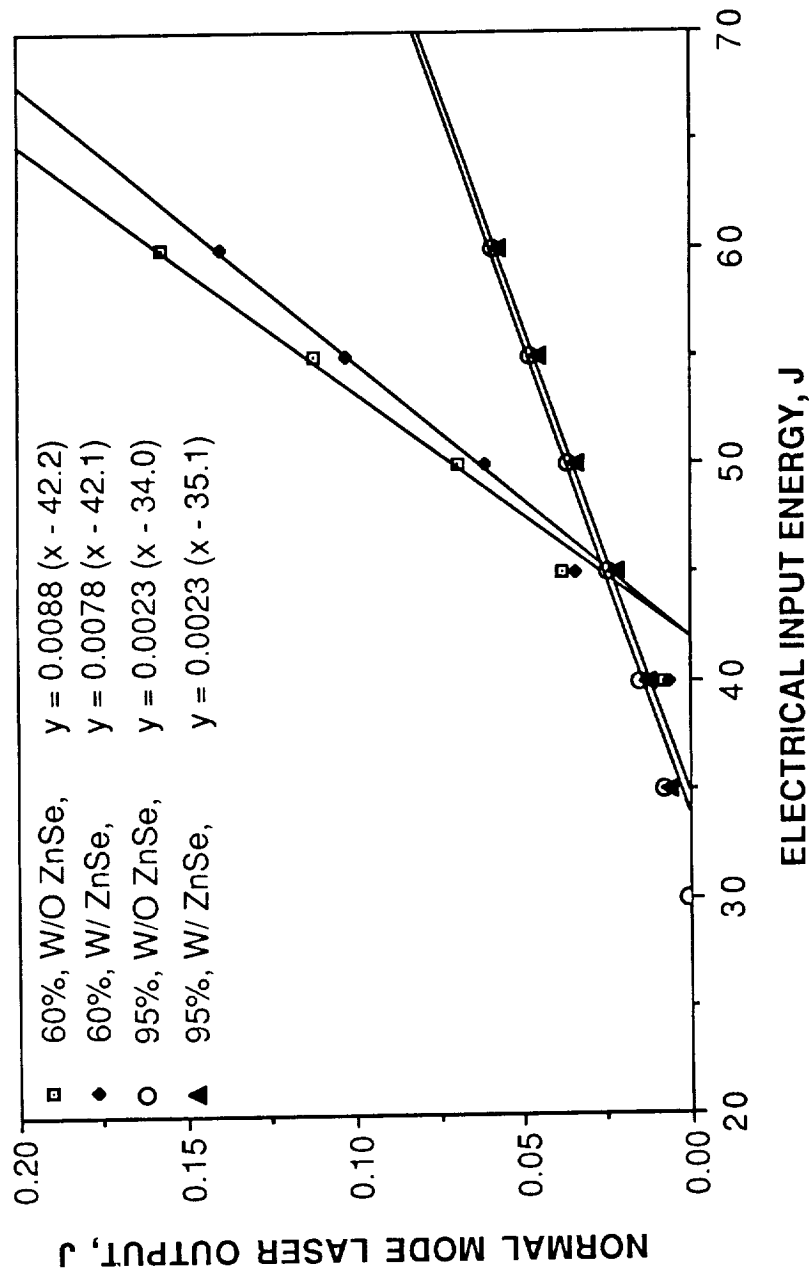


Figure 10. Loss coefficient measurement of ZnSe plate in a Ho:Er:Tm:YAG laser resonator with output mirrors of reflectivities of 60% and 95%.
 Ho:Er:Tm:YAG (0.02 Ho, 0.40 Er, 0.06 Tm), 5 mm x 90 mm rod, T=170 K, with a 10 MCC HR mirror, 146.5μF, 184μH, and pulse width of 300μs FWHM. Laser beam angle on the plate = 67.8 degree (Brewster angle).

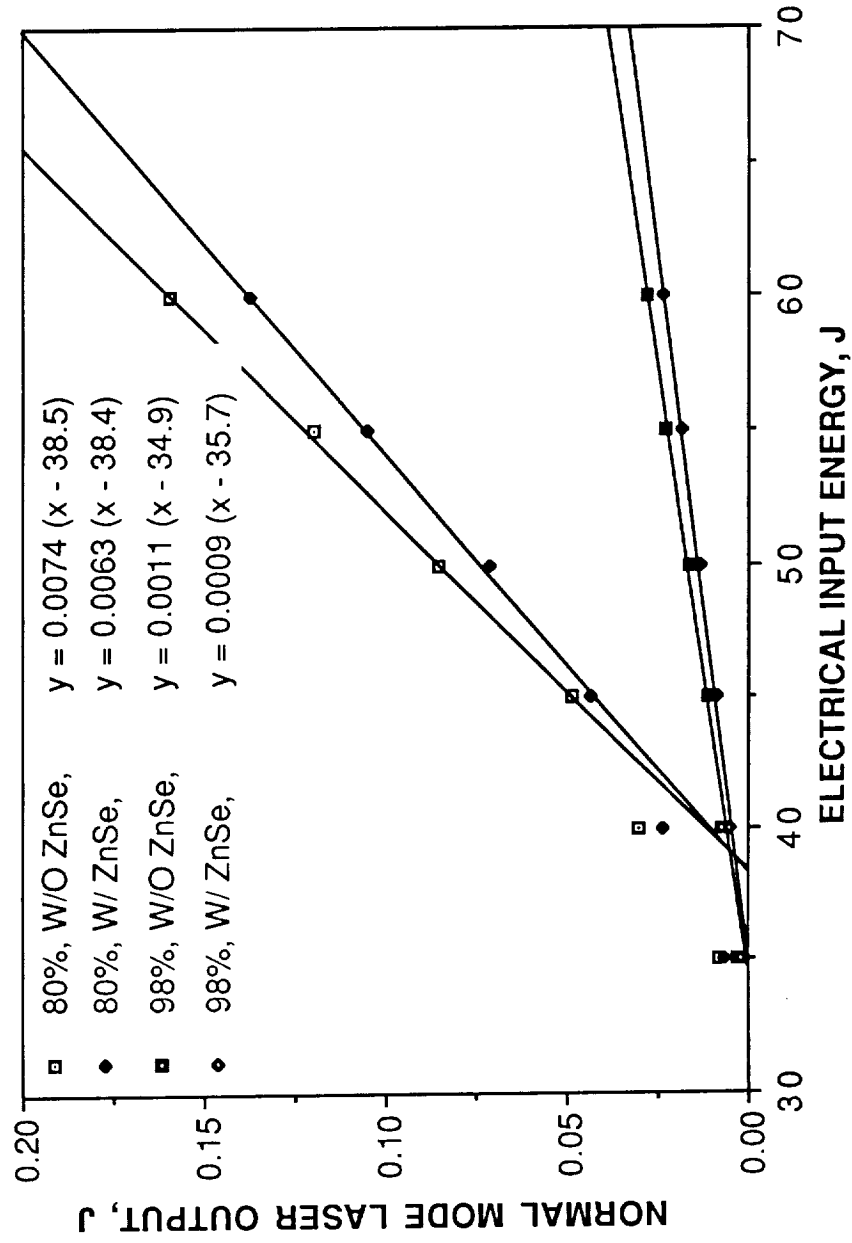


Figure 11. Loss coefficient measurement of ZnSe plate in a Ho:Er:Tm:YAG laser resonator with output mirrors of reflectivities of 80% and 98%.
Ho:Er:Tm:YAG (0.02 Ho, 0.40 Er, 0.06 Tm), 5 mm x 90 mm rod, $T=170$ K, with a 10 MCC Hr mirror, 146.5 μ F, 184 μ H, and pulse width of 300 μ s FWHM. Laser beam angle on the plate = 67.8 degree (Brewster angle).

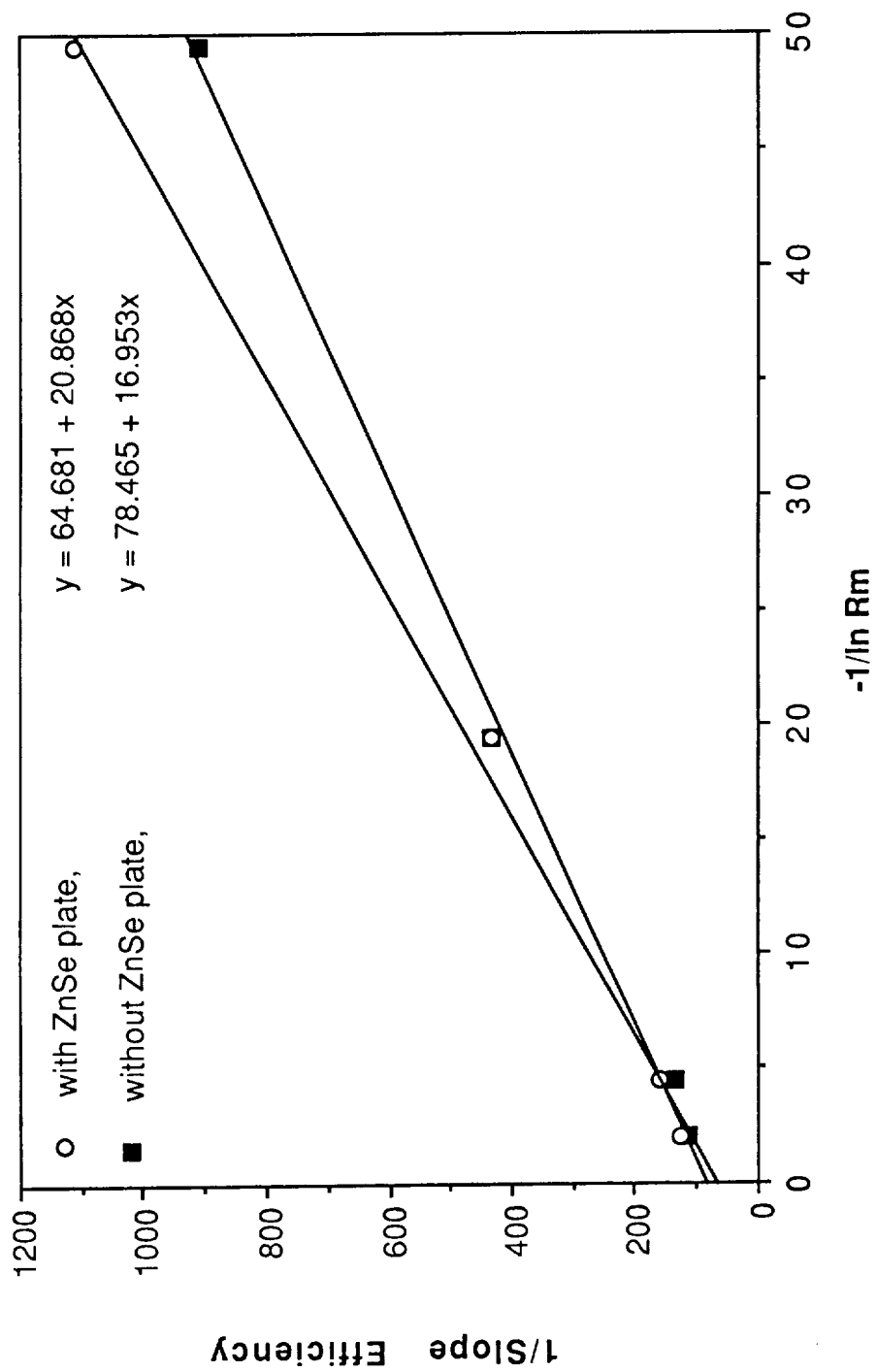


Figure 12. Inverse slope efficiency versus $-1/\ln R_m$ with and without ZnSe plate in a flashlamp-pumped Ho:Er:Tm:YAG Laser.

Appendix

Computer Programs for Pulse Forming Network Parameter Calculation

Computer Program for Multi-LC-Section Pulse Forming Network Design

```

10  PRINT "-----"
10  PRINT " "
20  PRINT " "
30  PRINT "      MULTISECTION PULSE FORMING NETWORKS      "
40  PRINT " "
50  PRINT "-----"
60  PRINT USING 330;"INPUT ", "PULSE ", "TOTAL ", "TOTAL ", " VOLT.", "SECTION", "SE
CTION", " RISE ", " PEAK ", "BLKBODY"
70  PRINT USING 330;"ENERGY", "WIDTH", "CAPACI.", "INDUCT.", " ", "CAPACI.", "I
NDUCT.", " TIME ", "CURRENT", " TEMP. "
80  PRINT USING 330;" J ", " usec ", " F ", " H ", " V ", " F ", "
H ", " usec ", " A ", " K "
90  S=7.62 ! ARC LENGTH ( cm )
100 D=.4 ! BORE DIAMETER ( cm )
110 FOR E=100 TO 500 STEP 100
120 I=0
130 PRINT "-----"
140 FOR To=200 TO 2000 STEP 200
150 ! E INPUT ENERGY
160 ! To PULSE DURATION
170 T=To*10-6 !PULSE DURATION ( sec )
180 Ko=4/3*S/D ! IMPEDENCE PARAMETER
190 Vo=2*(Ko2*E/T)(1/3) ! SUPPLY VOLTAGE
200 C=.5*(E*T2/Ko4)(1/3) ! TOTAL CAPACITANCE
210 L=.5*(T4*Ko4/E)(1/3) ! INDUCTANCE
220 Lo=L/3 ! SECTION INDUCTANCE
230 Co=C/3 ! SECTION CAPACITANCE
240 Rt=SQR(Lo*Co)/10-6 ! RISE TIME
250 Zo=SQR(L/C) ! IMPEDENCE
260 K0=(.5*Vo*Zo)(1/2) ! IMPEDANCE PARAMETER
270 Ia=.5*Vo/Zo ! LAMP CURRENT
280 Ip=Vo/(Zo+.02*S/(3.14*(D/2)2)) ! PEAK CURRENT
290 Ca=3.14*(D/2)2 ! CROSS SECTION
300 T=((9450*(D/100).03*(Ia/Ca).01)6+ (93*(D/100).27*(Ia/Ca).34)6)(1/6)
! TEMPERATURE
310 IF I=0 THEN PRINT USING 340;E,To,C,L,V0,Co,Lo,Rt,Ip,T
320 IF I<>0 THEN PRINT USING 350;To,C,L,V0,Co,Lo,Rt,Ip,T
330 IMAGE 6A,2X,6A,1X,7A,2X,7A,2X,7A,1X,7A,3X,7A,2X,5A,1X,6A,1X,7A
340 IMAGE 4D,2X,6D,2X,1D.DDE,2X,1D.DDE,2X,4D,2X,1D.DDE,2X,1D.DDE,2X,4D,2X,5D,3
X,6D
350 IMAGE 6X,6D,2X,1D.DDE,2X,1D.DDE,2X,4D,2X,1D.DDE,2X,1D.DDE,2X,4D,2X,5D,3X,6
D
360 I=1
370 NEXT To
380 NEXT E
390 PRINT "-----"
400 END

```

ORIGINAL PAGE IS
OF POOR QUALITY

Computer Program for Single-LC-Section Pulse Forming Network Design

```

10  PRINT "-----"
20  PRINT
30  PRINT "          FLASHLAMP PULSE FORMING NETWORK
40  PRINT
50  PRINT "-----"
60  PRINT USING 350;"PULSE  "," PULSE  ","CAPACI. ","INDUCT.  "," VOLT  ","EXPLO.
   "," LIFE  ","BLKBDY"," PEAK  "," PEAK  "
70  PRINT USING 350;"ENERGY  "," WIDTH  ","          ","          ","          ","ENERGY
   ","          "," TEMP. ","WAVELEN. ","CURRENT"
80  PRINT USING 350;" J  "," usec  "," F  "," H  "," V  "," J
   ","(10^6)"," K  "," nm  "," A  "
90  FOR Eo=100 TO 500 STEP 100
100  I1=0
110  PRINT "-----"
120  FOR To=100 TO 1000 STEP 100
130  T=To/3 !TIME CONSTANT
140  Ko=25 !IMPEDENCE PARAMETER
150  Ke=7.5E4 !EXPLOSION ENERGY CONSTANT
160  A=.8 !CRITICAL DAMPING
170  C=(2*Eo*A^4*(T*10^(-6))^2*Ko^(-4))^^(1/3) !CAPACITANCE (F)
180  L=(T*10^(-6))^2/C !INDUCTANCE (H)
190  V=(2*Eo/C)^(1/2) !VOLTAGE (V)
200  Ex=Ke*(T*10^(-6))^^(1/2) !EXPLOSION ENERGY
210  I=V^2/Ko^2 !CURRENT
220  Life=(Eo/Ex)^(-8.5)/10^6 !LIFE OF FLASH
230  Zo=SQR(L/C) !IMPEDANCE
240  Re=.02 !FLASH RESISTIVITY FOR 100us<t<1ms
250  Le=7.62 !ARC LENGTH(cm)
260  Bo=.4 !BORE DIAMETER(cm)
270  Rt=Re*Le/(3.14*(Bo/2)^2) !FLASH RESISTANCE
280  Ip=V/(Zo+Rt) !PEAK CURRENT
290  Ca=3.14*(Bo/2)^2 !CROSS SECTION (cm^2)
300  D=Bo/100 !BORE DIAMETER (m)
310  Te=((9450*D^.03*(I/Ca)^.01)^6+(93*D^.27*(I/Ca)^.34)^6)^(1/6) !TEMPERATURE
320  Wm=2.898E6/Te ! PEAK WAVELENGTH ( nm )
330  IF I1=0 THEN PRINT USING 360;Eo,To,C,L,V,Ex,Life,Te,Wm,Ip
340  IF I1<>0 THEN PRINT USING 370;To,C,L,V,Ex,Life,Te,Wm,Ip
350  IMAGE 6A,1X,6A,2X,7A,2X,7A,2X,5A,3X,6A,1X,6A,2X,7A,1X,8A,1X,7A
360  IMAGE 6D,1X,4D,2X,1D.DDE,2X,1D.DDE,2X,4D.D,1X,4D.D,2X,2D.DE,2X,4D,1X,6D.D,
2X,6D
370  IMAGE 7X,4D,2X,1D.DDE,2X,1D.DDE,2X,4D.D,1X,4D.D,2X,2D.DE,2X,4D,1X,6D.D,2X,
6D
380  I1=1
390  NEXT To
400  NEXT Eo
410  PRINT "-----"
420  PRINT "-----"
430  END

```